A Flight Control System Stability Study for a Guided System

Dr. Lester McCoy
Air Defense Systems Department
Raytheon – Integrated Defense Systems
Andover, MA, USA
Lester.McCoy@raytheon.com

John Beale
Operational Analysis and Simulation Department
Raytheon – Integrated Defense Systems
Andover, MA, USA
John_A_Beale@raytheon.com

Abstract – *This paper describes a flight control stability analysis performed for a guided missile system. The purpose of the study was to investigate autopilot stability of a new version of an existing missile design from the vibration analysis perspective. Missile body bending mode analysis of new missile telemetry data was analyzed and compared to historical data using analysis tools that were developed during a number of test events leading up to the first missile flight test. The study showed that the new missile was within family of the historical data and illustrates the importance of maintaining databases for future missions. This paper will discuss the analysis techniques used as well as the process for managing the results. Given the proprietary nature of the system, no missile test data will be presented in this paper. It will instead focus on the tools, methodology; lessons used in the study, and include example illustrations.*

Keywords: Modal Analysis, flight control stability, autopilot.

1 Introduction

An understanding of autopilot stability is important for any guided flight system. Instability due to sustained, undamped, high frequency oscillations can lead to catastrophic missile flight failures and there is a significant focus of effort to control them. Body bending modal analysis using Finite Element Methods and other structural analysis techniques are useful tools in the design and development stages of a guided flight system. Ground Vibration Survey (GVS) and Missile Stability and Frequency Response (MSFR) testing using a missile are performed during hardware integration and test. But modal analysis during post flight test reconstruction to investigate the presence of vibration anomalies that may have occurred during flight can also be performed. The purpose of this paper is to illustrate a practical application of modal analysis methods to investigate flight control stability for a guided missile system. Specifically, modal analysis is used to identify the missile resonant peaks and oscillations from the missile inertial sensor assembly (ISA) telemetry data for a number of historical missions for a basis of comparison to a new missile flight test. A new missile was a refresh of an existing missile design to deal with parts obsolescence.

This paper is organized as follows. Section 2 provides a brief description of the purpose of the modal analysis study. It includes a description of two past test events of the MSFR testing and (GVS) testing conducted on both a baseline legacy missile and new missile. These tests are used to determine the body bending modes and missile flight control system (FCS) stability margins. The results of the MSFR and GVS test events were used in the identification of missile resonances observed in the flight test data. A review of an example of a digital homing autopilot, a review of Fourier analysis, and the effects of quantization in the telemetry data are also described in Section 2. Section 3 describes the research methods of the study, which describe the parameters of interest and the analysis procedure. Section 4 describes the study results and how the analysis results were compiled, while conclusions and future work are discussed in Sections 5.

2 Background

This work was commissioned as part of a post flight reconstruction effort and deep dive activity for the first flight test of the new missile program. During this study, missile autopilot time responses were analyzed for anomalies and high frequency stability analysis was performed to investigate the impact of flexible body dynamics on autopilot stability for different stages of flight (initial launch, missile motor burn, midcourse and terminal). Instability is defined for this study as the presence of un-damped oscillations sustained for at least one second during any segment of flight.

2.1 MSFR and GVS Test Description and Results

The MSFR test was conducted to ensure that the final operational configuration of the missile hardware and software was stable with respect to the missile body lateral and torsional bending modes of vibration. The purpose of the MSFR test was to document the behavior of the missile in a simulated flight configuration without aerodynamic loading with an operational control actuator system (CAS), ISA, and onboard missile computer. The stimulus for the MSFR test is the CAS. The individual fins of the CAS are commanded with a sinusoidal chirp waveform which is

swept over a range of frequencies that include the lower body bending modes during open loop tests; fin step commands are used during closed loop tests. Open loop tests are used to characterize airframe transfer functions; closed loop tests are used to test system stability and observe stability margins. The missile is electrically activated during this test. Responses of the ISA gyros and accelerometers, autopilot commands, and the fin feedback positions are recorded during this test and analyzed. The gain and phase margins of the legacy missile were compared with the new missile, ensuring no anomalies.

Prior to MSFR testing, GVS testing was conducted to survey data of the flexible body modes by exciting the missile with electro-dynamic shakers and monitoring external response accelerometers located at predetermined locations on the missile. The electro-dynamics shakers are designed to stimulate the airframe with a low level, broad spectrum force at multiple locations along the missile body. The missile is not active during this test. Information gathered from the GVS was used in the comparison between the legacy and new build missile, as well as to update the systems engineering analytical models of the control system.

Collectively, the frequency and time domain response information determined from the GVS and MSFR provides a detailed characterization of the missile flexible bending of the airframe and autopilot stability at high frequencies. The MSFR test configuration is shown in Figure 1. The missile is suspended by bungee straps on each end with a safety strap loosely hung below. The hoist holds the spreader bar and is stabilized by counterweights on the bottom.

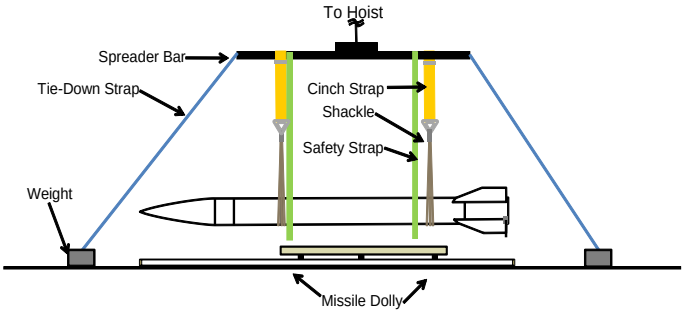

Figure1. MSFR Test Set-up

Autopilot stability for the closed loop MSFR tests is defined by the fins exhibiting a sustained oscillation. An unstable scenario will cause the fin deflections to increase until they reach a saturation limit. This limit is based on actuator current and hydraulic pressure limits within the CAS. Maximum fin rate was a metric for determining the stability of a gain margin test. The derivatives of the measured fin positions were utilized to determine the angular rate of the fin. Another indicator was the presence of sustained oscillations, most commonly at a single frequency.

2.2 Digital Homing Missile Autopilot Model

An autopilot for a modern homing missile converts guidance system acceleration commands into control surface actuator commands [2]. These actuators in turn produce deflections of the aerodynamic control surfaces that maneuver the missile. The lateral acceleration of a missile must be controlled over a wide range of flight conditions which affect the missile's stability and control effectiveness. A digital autopilot uses a set of constant control gains that are switched at prescribed flight conditions to control missile motion. A detailed description and derivation of the digital autopilot model is discussed in [2] and [3] and an example three-loop autopilot is shown in Figure 2 below. For the purpose of our study, the missile flexible body modes are represented in the Airframe blocks of Figure 2. The missile body bending frequencies and damping vary due to a number of factors including: temperature, fuel mass expended, the weight distribution of the missile's components, number of missile sections and their section joints/interfaces, and the location of instrumentation within the missile.

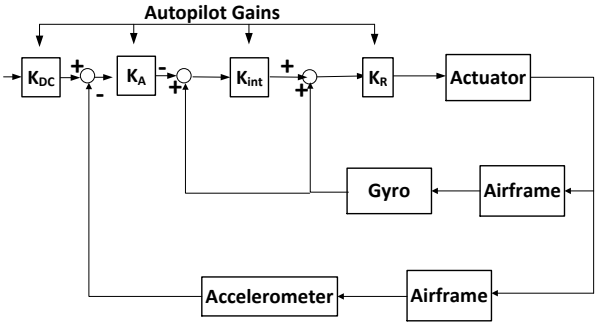

Figure 2. Flight Control System with Three Loop Autopilot

2.3 Fast Fourier Transform of a Signal

The fast Fourier transform (FFT) of a signal is described at length in [1]. For this study, scaling was applied to the transformed signal so that the magnitude axis scale represents the power spectrum. Equations 1 and 2 give the Discrete Fourier Transform for a signal of length M.

$$X(k) = \sum_{j=1}^{M} x(j)\omega_M^{(j-1)(k-1)} \tag{1}$$

$$x(j) = \left(\frac{1}{M}\right)\sum_{k=1}^{M} X(k)\omega_M^{-(j-1)(k-1)} \tag{2}$$

The term, ω_M, is the M^{th} root of unity and is given by

$$\omega_M = e^{(-2\pi i/M)}. \tag{3}$$

The transformed signal, *X(k)*, is scaled by a factor , *S*, where

$$S = \frac{2}{M}. \tag{4}$$

The numerator of the scale factor is used to account for the signal contribution from the negative frequency components of the signal in the spectrum, while M is used to normalize the basis vectors of the FFT. The scaled signal, X_S, now becomes

$$X_S = S \cdot X(k). \tag{5}$$

Consider sampling a signal composed of a 40 Hz sinusoid of amplitude 0.1 and a 100 Hz sinusoid of amplitude 0.05 in the presence of zero mean additive white noise. Samples are taken at 1000 Hz. Additional setup parameters are listed below. Sampling Frequency is given by:

$$F_S = 1000Hz \tag{6}$$

$$T = 1/F_s \tag{7}$$

$$M = 1000 \tag{8}$$

$$t = (0,1,\cdots M-1) * T \tag{9}$$

$$x = 0.1\sin(2\pi 40t) + 0.05\sin(2\pi 100t) \tag{10}$$

$$y = x + 2R \tag{11}$$

Where F_s is the sampling frequency, T is the sampling time, M is the signal length, t is the sampling time vector, x is the signal under evaluation, and y is the signal plus noise, and R is an array of random numbers with length M. Figure 3 shows the real and imaginary components of the FFT of y. Note that the frequency spectrum is symmetric for positive and negative frequencies, while Figure 4 shows the signal and its power spectrum [1].

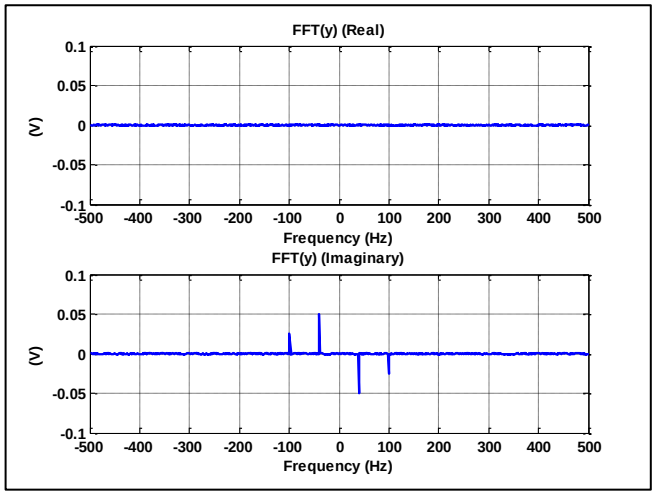

Figure 3. Signal Example - Time Domain

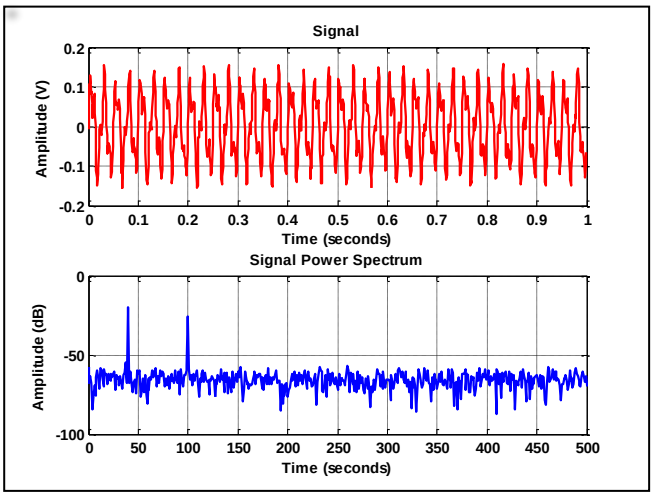

Figure 4. Signal and Power Spectrum

Observe that two resonant peaks at 40Hz and 100Hz are clearly shown in the frequency domain (Figure 2).

2.4 Quantization Effects

The missile telemetry contains digital samples of analog signals. As a result, quantization effects will be present in the data. The system under evaluation contained only 6 bit digital representations of many of the analog signals being analyzed. The signal levels due to the body bending effects in the accelerometers and gyros are an order of magnitude below the size of the quantization. For this reason, it was feared that structural resonances could not be observed in the data. However, the FFT did show the presence of the body bending modes. The reason for this is discussed below.

Quantization effects are commonly treated as noise in the data [1]. The error introduced by the quantization is typically uniformly distributed over the quantization level (Q). If the signal is dynamic and sweeps rapidly through the different quantization levels then the quantization error will appear to be uncorrelated from sample to sample. This allows the noise to be treated as "white" over the bandwidth of the sampled data. Figure 5 below is an example of quantization errors from a system with a quantization level of 1 Volt. This error is typical of the data under analysis. It is seen that there is correlation from sample to sample, which will cause the whiteness assumption to be challenged.

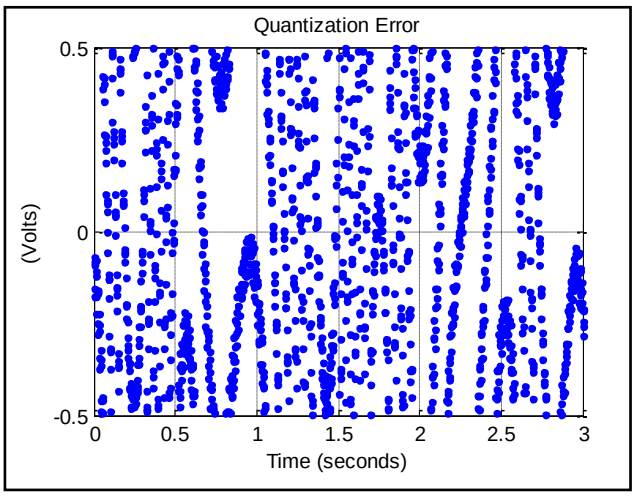

Figure 5. Quantization Error Illustration.

Figure 6 illustrates the histogram of a 100,000 sample example of the signal from figure 5. The probability density function (pdf) is very nearly uniform here and ideally will be 1across the quantization error.

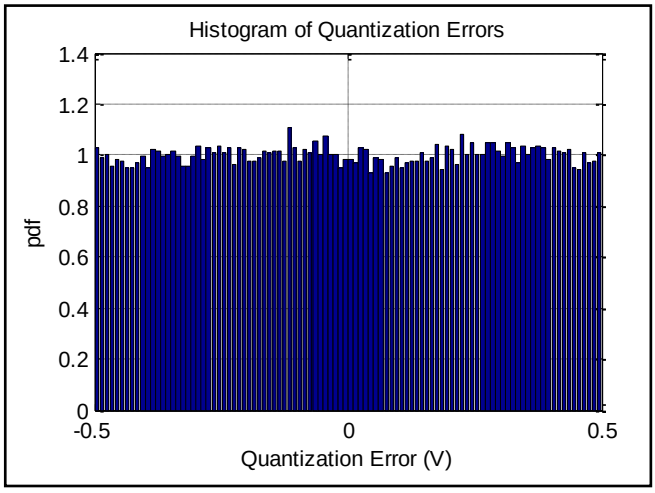

Figure 6. Example Quantization Error Histogram.

The expected signal to noise ratio (SNR) of a signal in the presence of quantization effects can be calculated as follows. Assuming the signal energy in the data is a sinusoid, the signal energy in the FFT is calculated as follows:

$$\begin{aligned} E_S &= \sum_{k=1}^{M} S_k^2 = \sum_{k=1}^{M} \left(S\cos((k-1)\omega T)\right)^2 \\ &= S^2 \sum_{k=1}^{M} \left(\frac{1}{2} + \frac{1}{2}\cos(2(k-1)\omega T)\right) \\ &= \frac{S^2}{2} \sum_{k=1}^{M} \left(1 + \cos(2(k-1)\omega T)\right) \\ &= \frac{S^2}{2}\left[M + \sum_{k=1}^{M} \cos(2(k-1)\omega T)\right] \end{aligned}$$

$$\cong \frac{MS^2}{2} \quad \text{assuming } \omega T \geq \frac{\pi}{M}, \quad N >> 1 \tag{12}$$

The noise has a variance as follows [1]:

$$\sigma_n^2 = \frac{Q^2}{12} \tag{13}$$

Since the noise is random it is treated in a statistical manner. The corresponding energy in the noise signal is as follows:

$$\begin{aligned} E[E_n] &= E\left[\sum_{k=1}^{M} n_k^2\right] = \sum_{k=1}^{M} E[n_k^2] \\ &= M\sigma_n^2 = \frac{MQ^2}{12} \end{aligned} \tag{14}$$

Since the noise energy is assumed to be white then it will be evenly distributed among all the FFT bins and the expected noise energy in each bin will be $\sigma_n^2 = Q^2/12$. The corresponding SNR becomes:

$$SNR = \frac{E_S}{\frac{E[E_n]}{M}} = \frac{MS^2}{2\left(Q^2/12\right)} = \frac{6*MS^2}{Q^2} \tag{15}$$

A simple example will be presented to illustrate these results. A test signal with features very characteristic of the live test data is illustrated in Figure 7.

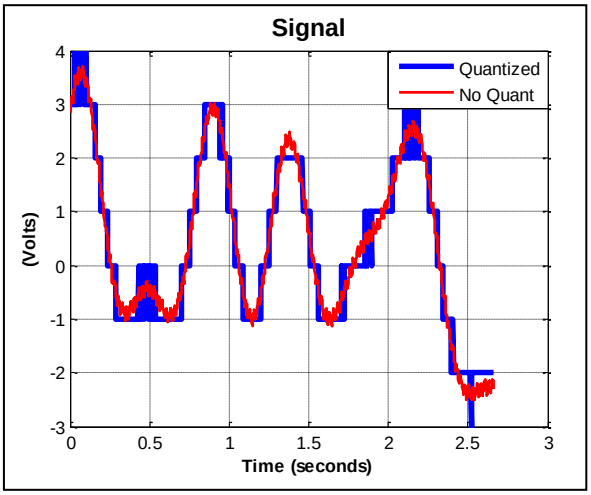

Figure 7. Example Signal with Gross Quantization.

The components of this signal as follows:

- A set of 20 sinusoids with amplitude .5 and random frequency and starting phase. Frequencies of the sinusoids uniformly distributed from 0 to 2.5 Hz.
- Two high frequency sinusoids at 40 Hz and 100 Hz and amplitudes .1V and .05V peak respectively simulating body bending signals.

- Quantization level of 1 Volt.
- 1333 Samples at 500 Hz.

The purposes of the low frequency sinusoids are to introduce a large signal that causes the total signal to extend across many quantization levels. Without this feature in the data the quantization error becomes highly correlated and does not appear as white noise in the spectrum. The body bending signal was deliberately chosen to be 20 times below the quantization level of 1 Volt to focus on the ability of the analysis to extract signals well below quantization levels.

Figure 8 illustrates exactly how the low amplitude sinusoid appears in the quantized data. At the levels where quantizer switches between two levels a high frequency toggling between two levels appears. This toggling effect is detected by the FFT and shows-up in the spectrum illustrated in Figure 9.

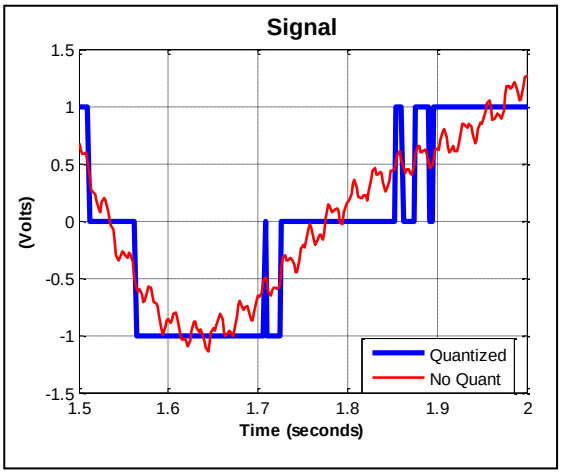

Figure 8. Example Signal Close-up.

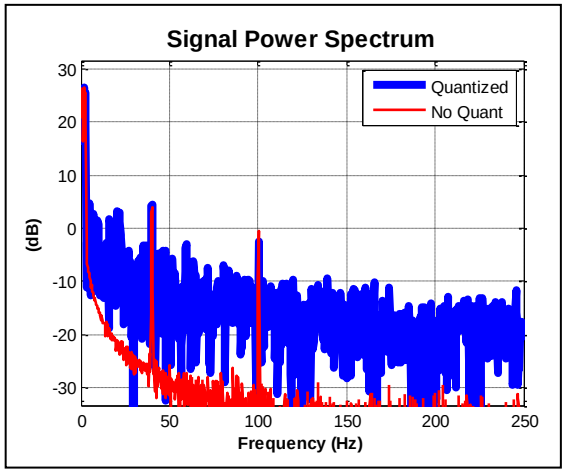

Figure 9. Spectrum of the Example Signal

The spectrum in figure 9 clearly illustrates the high frequency tone at 100 Hz. The noise spectrum does not appear to be strictly uniform in amplitude (not white) because of the correlation of the noise. A higher amplitude signal which rapidly extends across many quantization levels will have the effect of flattening out the noise spectrum. The SNR formula above predicts there will be a 13 dB signal peak above the average noise which is what appears in this figure.

3 Research Methods

A number of historical reports from past flight tests, MSFR tests, weight and center-of-gravity (CG) measurements, and GVS testing was compiled to determine a baseline for missile body bending mode frequencies of interest. Additionally, telemetry data from over 40 past flight tests was also analyzed to determine a baseline for comparison to the new missile. The results were presented to and reviewed by a team of subject matter experts.

The missile's telemetry data contains a number of analog signals of interest for the purpose of this FCS stability study. These are the measured missile body rates and accelerations vs. time from the ISA which are listed below.

- WM1 – Roll body rate
- WM2 – Yaw body rate
- WM3 – Pitch body rate
- NM1 – Longitudinal acceleration
- NM2 – Pitch Acceleration
- NM3 – Yaw acceleration

Table 1 lists typical missile body bending mode frequencies that were compiled from the source test reports and documentation.

Table 1. List of Missile Bending Mode Frequencies

Missile Bending Frequency	Frequency
First Bending Mode	A
Second Bending Mode	B
First Torsional Mode	C
Third Bending Mode	D
Aliased Gyro Spin Frequency	E

The telemetry data analysis procedure for this flight control stability study can be broken down into four distinct steps.

1. Perform an FFT of ISA outputs over the total flight time scaled by the missile data sampling rate.

2. Note the presence of small and larger tones in the missile body rates and accelerations (relative to spectrum envelope). Tones should be clearly observable above the surrounding noise.

3. Compare tone locations to the compiled list of interested frequencies from past test events.

4. Further investigate channel spectrums by autopilot band and flight phase timeframe (e.g. launch and post burnout, etc.)

Use of this process allowed the identification of vibration frequencies for each data set.

4 Results

The body bending modes of the new missile were sharper and more pronounced for certain modes than from some of the historical data. The historical data varied depending on production vintage, and so the new missile data matched some of the historical data exactly but not others. The first missile body bending mode frequency increases as the weight and cg shift as the rocket motor burns off fuel. No oscillations or other anomalies were observed in the new missile test data. The analysis result for all of the available data was summarized into a chart similar to what is displayed in Table 2. Note that the table contains only a representation of reported data and does not contain any real technical data. Numerous plots of data to illustrate baseline performance were created for comparison with the first new missile flight test, similar to those that were shown in Figure 9.

Table 2. Sample Spectral Analysis Results

Frequency	% of FTs Observed	Mission A	Mission B
First Bending Mode	X	■X●Y	■X●Y
Second Bending Mode	X		
First Torsional Mode	X	■X ●Y	■X●Y
Third Bending Mode	X		
Gyro Spin Frequency Aliasing	X	■X	■Y
Undocumented Frequency A	X	■X	
Undocumented Frequency B	X		●Y
Table Legend: ●Y : peak present in acceleration spectrum channel ■X : peak present in rate spectrum channel			

5 Conclusions

The Flight Control Stability Study provided new insight into FCS performance during flight tests. It was shown that modal analysis can be used to identify the missile resonant peaks and oscillations from the test ISA data. A database of missile body bending mode from numerous past flight tests was created for comparison to future missions. As a result of this study, body bending mode analysis has been incorporated as standard practice for pre-mission and post mission flight test work, This analysis has since been performed on subsequent flight tests of the new missile as well as legacy missile flights.

The new missile flight control system stability was found to be within family of the previous missiles based on available data. No frequencies or behaviors were observed that were not seen in past successful missions. Deep dive of mission data performed on new missile test data during each flight phase: launch, pre/post burnout, and homing phase, revealed a clear migration of 1st bending mode from launch through burnout as expected. This phenomenon was also observed during the MSFR testing.

5.1 Future Work

Among areas of future work is the continued refinement of the pre-mission and post-mission flight test analysis suite to ensure that no critical items are overlooked. For example, several missile resonance peaks were observed in the legacy data that were not seen in previous ground testing of missiles at known frequencies. Further investigation is required to resolve the root cause of this unknown frequency; however these were not seen in any of the new missile test data.

Acknowledgment

The authors would like to thank Michael M. Hart and Aaron Spettel for sponsoring this effort and their hours of technical support and review. We would also like to acknowledge the Raytheon Integrated Defense Systems (IDS) Systems, Validation and Test Directorate (SVTAD) and the Systems Architecture, Design and Integration Department (SADID) for funding and collaboration.

References

[1] A.V. Oppenheim and R.W. Schaffer, *Discrete Time Signal Processing*, Prentice-Hall, 1999.

[2] F.W. Nesline and N.C. Nabbefeld, *Design of Digital Autopilots for Homing Missiles, Nesline,* In Proceedings of American Control Conference, San Diego, California, 1979.

[3] P. Zarchan, *Tactical and Strategic Missile Guidance, Fifth Edition*, AIAA, Reston, VA, 2007.